SciMedCentral
JSM Diabetology and Management

Review Article

Effect of Streptozotocin-Induced Type 1 Diabetes Mellitus on Contraction and Calcium Transport in the Rat Heart

Frank Christopher Howarth[1]*, Lina AlKury[2], Manal Smail[1], Muhammad Anwar Qureshi[1], Vadym Sydorenko[3], Anatoliy Shmygol[1], Murat Oz[4], and Jaipaul Singh[5]

[1]*Department of Physiology, UAE University, UAE*
[2]*Department of Health Sciences, Zayed University, UAE*
[3]*Department of Cellular Membranology, Bogomoletz Institute of Physiology, Ukraine*
[4]*Department of Basic Medical Sciences, Qatar University, Qatar*
[5]*School of Forensic & Applied Sciences, University of Central Lancashire, UK*

***Corresponding author**

Frank Christopher Howarth, Department of Physiology, College of Medicine & Health Sciences, P.O. Box 17666, Al Ain, UAE University, UAE, Tel: 0097137137536; Email: chris.howarth@uaeu.ac.ae

Submitted: 16 September 2017

Accepted: 28 September 2017

Published: 29 September 2017

Keywords

- Streptozotocin
- Diabetes mellitus
- Rat
- Cardiomyopathy
- Heart
- Ventricle
- Calcium signaling
- Contraction

Abstract

Diabetes mellitus (DM) is a major global health disorder currently affecting 450 million people. Diabetic cardiomyopathy (DC) is a disorder of cardiac muscle that is independent of coronary artery disease and that may lead to heart failure in diabetic patients. The precise mechanism(s) of diabetic cardiomyopathy are still not fully understood. Therefore, it is of paramount importance to develop experimental models of DM to study the time course and cellular, subcellular and molecular mechanisms of diabetic cardiomyopathy. With this in mind, scientists initially discovered that the antibiotic, streptozotocin (STZ) could be used to rapidly to induce diabetes mellitus in animal models. STZ destroys pancreatic beta cells, leading to hypoinsulinemia and hyperglycaemia. If left untreated hyperglycaemia may lead to DC and eventually heart failure. Initially in DM, the cardiac myocytes become apoptotic, disorganised and the number of myocytes are significantly reduced. The heart responds by enlarging itself (hypertrophy) which is accompanied by fibrosis leading to a physiological remodelling process. Within the myocytes, the process of excitation-contraction coupling (ECC) is deranged. This is due to an inability of the heart cells to regulate Ca2+ which is the initiator and regulator of cardiac muscle contraction. As a result, the heart takes longer to contract and to relax leading to DC, progressive heart failure and eventually sudden cardiac death. The aim of this review was to evaluate our current understanding of contractile dysfunction and disturbances in Ca2+ transport in the STZ-induced diabetic rat heart.

ABBREVIATIONS

DM: Diabetes Mellitus; DC: Diabetic Cardiomyiopathy; STZ: Streptozotocin; ECC: Excitation-Contraction Coupling; SR: Sarcoplasmic Reticulum; SERCA2: Sarcoplasmic Reticulum Ca^{2+} ATPase Pump; TPK: Time to Peak; THALF: Time to Half; EPI: Epicardial; ENDO: Endocardial; DNA: Deoxyribonucleic Acid; mRNA: Messenger Ribonucleic Acid; RYR: Ryanodine Receptor

INTRODUCTION

The STZ-induced diabetic rat is a widely used experimental model of DM. STZ selectively enters pancreatic beta cells via the GLUT2 glucose transporter where it causes damage to the genetic machinery and ultimately leads to beta cell death [1]. The general characteristics of the STZ-induced diabetic rat include hypoinsulinemia, hyperglycemia, dyslipidemia, polyuria, reduced body weight gain, polydipsia and polyphagia [2]. Contractile dysfunction, which is frequently observed in the diabetic heart, may include disturbances in heart rate, stroke volume, cardiac output, ejection fraction and rates of pressure development and relaxation rate [3-7].

Experiments performed in ventricular myocytes isolated from diabetic heart have variously displayed either unaltered or reduced amplitude of shortening, and prolonged time course of contraction and relaxation [8-11]. Intracellular free Ca^{2+} $[Ca^{2+}]_i$ transport systems are essential to the initiation and regulation of cardiac myocyte contraction and relaxation. During the process of ECC, the arrival of an action potential at a ventricular myocyte causes membrane depolarization leading to the opening of voltage-gated L-type Ca^{2+} channels and a small influx of Ca^{2+}. This small entry of Ca^{2+} triggers a much larger release of Ca^{2+} from the sarcoplasmic reticulum (SR). There follows a transient rise in intracellular Ca^{2+} (Ca^{2+} transient) which binds to the troponin C and initiates and regulates the process of myocyte contraction. Relaxation of contraction begins when Ca^{2+} is pumped back into the SR via the SR Ca^{2+} ATPase pump (SERCA2) and effluxed from the cell, primarily via the Na^+/Ca^{2+} exchanger [12-14]. Experiments performed in cardiac myocytes from diabetic heart have variously displayed disturbances in Ca^{2+} transient, time course of Ca^{2+} transient, L-type Ca^{2+} current, SR Ca^{2+} content, uptake and release and Na^+/Ca^{2+} exchange current[5,15-18]. The aim of this review was to evaluate our current understanding of contractile dysfunction and disturbances in Ca^{2+} transport in the STZ-induced diabetic rat heart.

Diabetogenic Action of Streptozotocin

The general chemical structure of STZ is shown in Figure 1. STZ is an antimicrobial agent which has also been used as a chemotherapeutic alkylating agent [19,20]. STZ is typically administered dissolved in a citrate buffer by either intraperitoneal or intravenousinjection. Once in the blood circulation, STZ travels to the pancreas where it selectively accumulates in pancreatic beta cells via the low-affinity GLUT2 glucose transporter in the plasma membrane. It should be noted that STZ is also able to damage other organs that express GLUT2 including the kidney and the liver [21,22]. It is generally believed that the toxicity of STZ is dependent upon the DNA alkylating activity of its methylnitrosourea moiety and methylation of the DNA molecule. Transfer of the methyl group from STZ to the DNA molecule causes damage and fragmentation of the DNA. Beta cell toxicity might also arise from the action of reactive oxygen species [1,23]. Whatever the mechanism(s) of action, the consequences of STZ treatment are damage to the beta islet cells of the pancreas and a reduction in the ability of these cells to produce insulin (Figure 2). The nature of the pathophysiological effects of STZ depends to a large extent on the dose and duration of treatment.

Blood Chemistry in the Streptozotocin-Induced Diabetic Rat

The general characteristics of the STZ-induced diabetic rat include hypoinsulinemia, hyperglycemia, polyuria, decreased body weight gain, polydipsia and polyphagia [2]. Insulin levels fall dramatically in diabetic rats compared to controls (Table 1). Due to the falling concentrations of insulin, target organs like the liver and muscle are unable to clear glucose from the blood circulation and blood glucose rises. Following a 45-60 mg/kg body weight injection of STZ in adult rats the blood glucose levels typically rise to an average of 400 mg/dl in STZ treated rats compared to 100 mg/dl in controls (Table 2). Urine glucose is also elevated in diabetic rats [24] compared to controls. Persistently elevated levels of glucose in the blood of diabetic rats causes glycosylation of hemoglobin and glycosylated hemoglobin is a widely used diagnostic criterion for DM (Table 3). Glycosylated hemoglobin can rise to an average of 8.5% in diabetic rats compared to 4.0 % in controls (Table 3). Alterations in lipid profile including increased cholesterol [7], increased free fatty acids [7], increased atrial and brain natriuretic peptides[10,25], reduced insulin-like growth factor-1 and triiodothyronine [7,26], increased creatine

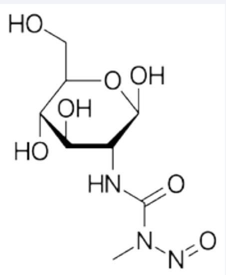

Figure 1 Diagram showing the chemical structure of streptozotocin.

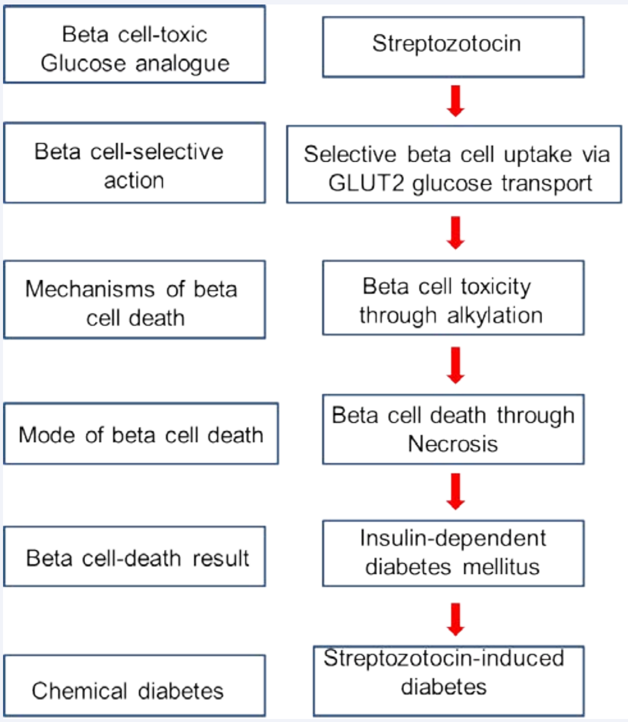

Figure 2 A schematic diagram showing the toxic effects of streptozotocin in beta cells. Adapted from Lenzen, 2008(1).

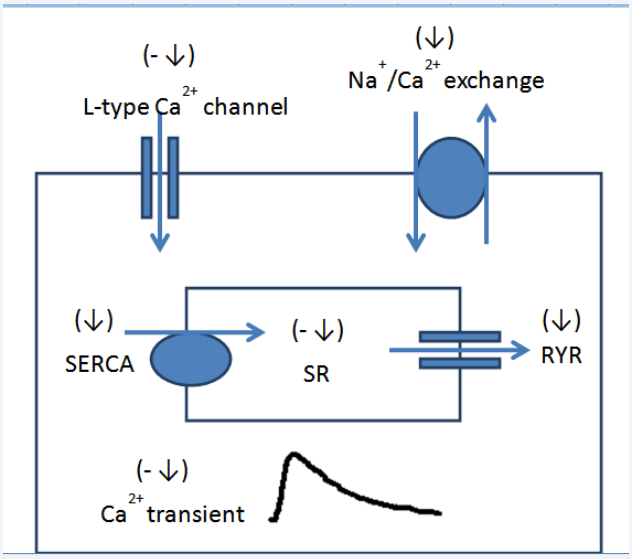

Figure 3 Diagram showing the proposed actions of STZ-induced diabetes on Ca2+ transport systems in the ventricular myocyte. -=No effect, ↓=Reduced activity, ↑=Increased activity.

[27], and increased blood osmolarity also occur in diabetic animals compared to controls [28,29].

Body and Heart Weight in the Streptozotocin-Induced Diabetic Rat

Body weight gain is typically reduced in diabetic rats compared to controls (Table 4). Heart weight is typically reduced

Table 1: Blood insulin levels in the streptozotocin-induced diabetic rat			
Dose of STZ (mg/kg body weight)	**Treatment time**	**Insulin level (Control vs. STZ)**	**Reference**
55 iv	6 w	43.3 vs. 31.3 μU/ml	[44]
65 iv	15, 27 d	31.2 vs. 12.4 15 d, 13.1 27 d μU/ml	[7]
55 ip	7 w	1.08 vs. 0.29 ng/ml	[5]
45-50 ip	7-8 w	1.98 vs. 0.27 ng/ml	[4]
65 iv	8 w	157 vs. 45 pmol/L	[64]
45 ip	8 w	1.2 vs. 0.3 ng/ml	[6]
45	8 w	1.12 vs. 0.3 ng/ml	[37]
60 ip	8-12 w	20.63 vs. 4.80 ng/ml	[29]

Table 2: Blood glucose levels in the streptozotocin-induced diabetic rat.			
Dose STZ (mg/kg body weight)	**Treatment time**	**Glucose level (Control vs. STZ)**	**Reference**
60 ip	3d, 30 d	70 vs. 265, 77 vs. 309 mg/dl	[40]
100 iv	4-6 d	96 vs. 329 mg/dl	[50]
65 ip	5-7 d	270 vs. 529 mg/dL	[51]
60 ip	1 w	128.6 vs. 479.0 mg/dL	[49]
65 iv	7 d	126 vs. 509 mg/dL	[52]
65 iv	7 d	6.9 vs. 27 mmol/L	[27]
65 iv	15 d,27 d	130 vs. 388 15 d, 130 vs. 435 27 d mg/dL	[7]
40 ip	28 d	3.40 vs.28.78 mmol/l	[36]
40 iv	3-4 w	10.3 vs. 40.4 mM	[61]
40 ip	4 w	3.40 vs. 28.78 mmol/L	[36]
50 ip	4-5 w	10.08 vs. 48.05 mmol/L	[56]
60 iv	4-6 w	163.2 vs. 511.3 mg/dL	[60]
50 iv	4-7 w	217 vs. 529 mg/dL	[55]
60 ip	4-10 w	92.4 vs. 407.5 mg/dL	[16]
60 ip	4 w,24 w	76 vs. 292, 66 vs. 252 mg/dl	[3]
50 ip	5 w	101 vs. 458 mg/dL	[57]
50 ip	5 w	105 vs. 421 mg/dL	[17]
55 iv	6 w	6.2 vs. 19.1 mmol/L	[44]
55 iv	7 w	94 vs. 333 mg/dL	[26]
55 ip	7 w	4.9 vs. 21.2 mmol/L	[5]
45-50 ip	7-8 w	7.2 vs. 22.8 mmol/L	[4]
60 ip	8 w	104.06 vs. 469.64 mg/dl	[65]
60 ip	8 w	98.00 vs. 440.38 mg/dl	[66]
45	8 w	5.2 vs. 22.6 mmol	[37]
60 ip	8 w	70.1 vs. 307.2 mg/dl	[48]
65 iv	8 w	180 vs. 546 mg/dl	[64]
55	8 w	105 vs. 344 mg/dl	[50]
45	8 w	5.2 vs. 22.6 mmol/L	[37]
55 iv	8 w	110 vs. 348 mg/dL	[45]
50 ip	8 w	116.6 vs. 386.8 mg/dL	[41]
45 iv	8 w	6.2 vs. 20.8 mmol/L	[6]
60 iv	8 w	4.7 vs. 30.8 mmol/L	[30]
65 iv	8 w	155 vs. 473 md/dL	[35]
60 ip	8w	70.1 vs. 307.2 mg/dL	[48]

60 ip	8-12 w	69.4 vs. 322.5 mg/dl	[43]
60 ip	8-12 w	92.4 vs. 407/5 mg/dl	[29]
60 ip	8-12 w	71.83 vs. 308.23 mg/dl	[47]
60 ip	8-12 w	78.3 vs. 366.7 mg/dL	[28]
60 ip	8-12 w	70.0 vs. 331.5 mg/dL	[46]
60 ip	8-12 w	71.83 vs. 308.23 mg/dL	[47]
60 ip	8-12 w	92.4 vs. 407.5 mg/dL	[29]
60 ip	8-12 w	68.0 vs. 347.4 mg/dL	[10]
60 ip	8-12 w	69.4 vs. 322.5 mg/dL	[43]
60 ip	9 w	70.50 vs. 260.17 mg/dL	[59]
60 ip	9 w	90.21 vs. 529.21 mg/dL	[38]
60 ip	12 w	7.57 vs. 19.47 mmol/L	[39]
60 ip	12 w	90.5 vs. 455.0 mg/dL	[11]
60 ip	13-24 w	110 vs. 554 mg/dl	[49]

Table 3: Glycosylated hemoglobin in the streptozotocin-induced diabetic rat.

Dose STZ (mg/kg body weight)	Treatment time	Glucose level (Control vs. STZ)	Reference
45-50 ip	7-8 w	3.9 vs. 8.3 %	[4]
55 ip	7 w	4.1 vs. 8.4 %	[5]
45 iv	8 w	3.3 vs. 8.3 %	[6]
45	8 w	4.3 vs. 8.9 %	[37]

Table 4: Body weight in the streptozotocin-induced diabetic rat.

Dose STZ (mg/kg body weight)	Treatment time	Body weight (Control vs. STZ)	Reference
100 iv	4-6 d	237 vs. 190 g	[50]
65 ip	5-7 d	370 vs. 269 g	[8]
65 ip	5-7 d	370 vs. 269 g	[51]
60 ip	7 d	282.1 vs. 237.2 g	[49]
65 iv	7 d	334.4 vs. 285.5 g	[27]
65 iv	7 d	351 vs. 279 g	[52]
40 ip	28 d	265 vs. 202 g	[36]
60 ip	30 d	314 vs. 238 g	[40]
50 ip	4-5 w	256.32 vs. 186.12 g	[56]
60 iv	4-6 w	420 vs. 239 g	[60]
50 iv	4-7 w	425 vs. 233 g	[55]
60 ip	4-10 w	385.4 vs. 233.8 g	[16]
60 ip	4, 24 w	305 vs. 248, 410 vs. 308 g	[3]
50 ip	5 w	240.2 vs. 196.8 g	[17]
50 ip	5 w	249.2 vs. 197.8 g	[57]
55 iv	6 w	448 vs. 335 g	[44]
55 iv	7 w	434 vs. 293 g	[26]
55 ip	7 w	366.6 vs. 270.6 g	[5]
45-50 ip	7-8 w	416.5 vs. 329.8 g	[4]
60 ip	8 w	352.25 vs. 267.57 g	[65]
60 ip	8 w	351.05 vs. 259.05 g	[66]
45	8 w	393.0 vs. 289.1 g	[37]

60 ip	8 w	312.0 vs. 229.1 g	[48]
65 iv	8 w	467 vs. 258 g	[64]
55 iv	8 w	380 vs. 285 g	[50]
55 iv	8 w	411 vs. 310 g	[45]
45 iv	8 w	422.5 vs. 312.8 g	[6]
60 iv	8 w	438 vs. 247 g	[30]
65 iv	8 w	462 vs.270 g	[35]
60 ip	8-12 w	304.3 vs. 221.1 g	[43]
60 ip	8-12 w	381.4 vs. 232.8 g	[29]
60 ip	8-12 w	326.83 vs. 226.23 g	[47]
60 ip	8-12 w	269.1 vs. 209.9 g	[46]
60 ip	8-12 w	300.6 vs. 224.0 g	[10]
60 ip	8-12 w	307.1 vs. 232.8 g	[28]
60 ip	9 w	351.20 vs. 198.80 g	[38]
60 ip	9 w	285.33 vs. 229.33 g	[59]
60 ip	12 w	589.83 vs. 256 g	[39]
60 ip	12 w	361.5 vs. 255.8 g	[11]
60 ip	13-24 w	426 vs. 266 g	[49]

but may occasionally be unaltered in diabetic rats (Table 5). Heart weight to body weight ratio is generally increased indicating a sign of hypertrophy but may also be unaltered in diabetic rats compared to controls (Table 6). Other studies have reported unaltered heart weight to tibial length [30], reduced left ventricle weight [31,32] and increased left ventricle to body weight ratio [33] in diabetic rats compared to controls. These data provide evidence of cardiac hypertrophy in the STZ-induced diabetic rat.

Hemodynamic Function *In vivo* and in the Isolated Perfused Heart of the Streptozotocin-Induced Diabetic Rat

Measures of hemodynamic function are shown in Table 7. Echocardiographic and other techniques have generally reported reduced heart rate [3-6,32,34,35,35-38] but sometimes unaltered heart rate [7,39] in diabetic rats compared to controls (Table 7). Associated with the changes in heart rate electrophysiological measurements of QRS, QT, PQ and PR intervals are generally prolonged [4,5,35,40] and sometimes unaltered [3,35,40] in diabetic rats compared to controls. Cardiac output may either be reduced or unaltered [4-6], stroke volume may be reduced or unaltered [4-6] and ejection fraction was generally reduced [5,6,32,37-39] but may also be unaltered [41] in diabetic rats compared to controls. Percentage fractional shortening was reduced [4-6,32,37-39] in diabetic rat. Left ventricular systolic pressure was reduced [33,35,36,39,42] and left ventricular diastolic pressure was increased [33,35-37,39,42] in diabetic rats compared to controls. Rates of pressure development and decline were lower [5,31,33,35-37,39] in diabetic rat. In the isolated perfused heart the spontaneous heart rate was lower [9,43], rates of pressure development and decline were lower [9] and the time to peak (TPK) and half relaxation (THALF) of pressure were prolonged [9] in diabetic rat heart. Collectively, these *in vivo* and *in vitro* experiments provide evidence of disturbances in hemodynamic function including heart rate, left ventricular systolic and diastolic pressure, rate of pressure development and decline, and cardiac output in the STZ-induced diabetic rat heart compared to controls.

Contraction in Ventricular Myocytes from Streptozotocin-Induced Diabetic Rat

The characteristics of ventricular myocyte contraction are shown in Table 8. Generally, ventricular myocytes are isolated from heart using a combination of enzymatic and mechanical dispersal techniques [9,16]. The viability, calculated as the percentage of rod shaped compared to round shaped myocytes, was generally lower [4,16,29,44] in myocytes isolated from diabetic rats compared to controls. Resting cell length was generally unaltered [4,5,10,11,28,43,45-49], but sometimes reduced [27] in ventricular myocytes from diabetic rats compared to controls. Cell width was either unaltered [28] or reduced [27], cell thickness was unaltered [27], surface area was increased [10] and calculated cell volume may be unaltered [28] or reduced [27] in myocytes from diabetic rats compared to controls. A recent study reported unaltered length in epicardial (EPI) and endocardial (ENDO) ventricular myocytes from diabetic rat [11]. The time course of shortening was prolonged [4,5,8-11,26,28,29,43,45-51] and the time course for half relaxation was either prolonged [4,5,8,9,11,26,43,45,46,50-52] or unaltered [10,28,29,47-49] in myocytes from diabetic rats compared to controls. A recent study reported prolonged TPK shortening in EPI and ENDO myocytes and prolonged THALF relaxation of shortening in ENDO but not in EPI left ventricular myocytes from STZ-induced diabetic rat [11]. Rate of development of shortening may be reduced [4,5,9,26,37] or unaltered [45,52] and the rate of decline of shortening may also be reduced [4,5,9,26,37] or unaltered [45,52] in myocytes from diabetic rats compared to controls. Amplitude of shortening may be reduced [4,5,9,26,27,37] or unaltered [8,10,11,28,29,43,45-49] in myocytes from diabetic rat. Increasing frequency of stimulation produces a negative staircase effect that was unaltered in myocytes from STZ-

Table 5: Heart weight in the streptozotocin-induced diabetic rat.

Dose STZ (mg/kg body weight)	Treatment time	Heart weight (Control vs. STZ)	Reference
65 ip	5-7 d	1.10 vs. 0.92 g	[8]
65 ip	5-7 d	1.10 vs. 0.92 g	[51]
65 iv	7 d	1.10 vs. 0.90 g	[52]
50 iv	4-7 w	1.35 vs. 0.88 g	[55]
60 ip	4-10 w	1.1 vs. 1.0 g	[16]
50 ip	5 w	4.04 vs. 4.08 mg/g	[57]
55 iv	7 w	1.85 vs. 1.37 g	[26]
55 ip	7 w	1.2 vs. 1.0 g	[5]
45-50 ip	7-8 w	1.25 vs. 0.97 g NSD	[4]
60 ip	8 w	1.2 vs. 1.06 g	[65]
60 ip	8 w	1.18 vs. 1.05 g	[66]
55 iv	8 w	1.54 vs. 1.29 gNSD	[45]
45 iv	8 w	1.3 vs. 1.0 g	[6]
60 iv	8 w	1.60 vs. 1.24 g	[30]
65 iv	8 w	1.04 vs. 0.74 g	[35]
60 ip	8-12 w	1.17 vs. 1.01 g	[43]
60 ip	8-12 w	1.1 vs. 1.0 g	[29]
60 ip	8-12 w	1.25 vs. 0.99 g	[47]
60 ip	8-12 w	1.17 vs. 1.04 g	[46]
60 ip	8-12 w	1.25 vs. 1.02 g	[10]
60 ip	8-12 w	1.21 vs. 1.04 g	[28]
60 ip	9 w	1.86 vs. 1.00 g	[38]
60 ip	12 w	780 vs. 595.1 mg	[39]
60 ip	12 w	1.13 vs. 0.96 g	[11]
60 ip	13-24 w	1.33 vs. 1.05 g	[49]

NSD=No significant difference

Table 6: Heart weight to body weight ratio in the streptozotocin-induced diabetic rat.

Dose STZ (mg/kg body weight)	Treatment time	Heart weight to body weight ratio (Control vs. STZ)	Reference
65 ip	1-7 d	3.05 vs. 3.03 mg/g NSD	[8]
65 ip	5-7 d	3.03 vs. 3.05 mg/gNSD	[51]
65 iv	7 d	3.12 vs. 3.21 mg/g	[52]
50 iv	4-7 w	3.16 vs. 3.81 mg/g	[55]
55 iv	7 w	4.33 vs. 5.23 mg/gNSD	[26]
55 ip	7 w	3.3 vs. 3.7 mg/g	[5]
60 ip	8 w	3.42 vs. 4.00 mg/g	[65]
60 ip	8 w	3.38 vs. 4.11 mg.g	[66]
55 iv	8 w	3.74 vs. 4.16 mg/g	[45]
45 iv	8 w	3.1 vs. 2.9 mg/gNSD	[6]
60 iv	8 w	3.7 vs. 5.3 mg/g	[30]
65 iv	8 w	2.25 vs. 2.74 mg/g	[35]
60 ip	8-12 w	4.41 vs. 5.04 mg/g	[46]
60 ip	8-12 w	4.28 vs. 4.71 mg/gNSD	[10]
60 ip	9 w	5.43 vs. 5.07 mg/gNSD	[38]
60 ip	12 w	3.13 vs. 3.78 mg/g	[11]
60 ip	13-24 w	3.14 vs. 3.97 mg/g	[49]

NSD=No significant difference

induced diabetic rat compared to control [26,45]. Spontaneous contractions (arrhythmic contractions) were increased in myocytes from diabetic rat [2]. Experiments in sarcomeres have reported reduced fractional shortening, decreased maximal rate of shortening and re-lengthening in diabetic rats compared to controls [31]. Collectively, these experiments provide evidence of disturbances in the time course of shortening, relaxation of shortening, and amplitude of shortening in ventricular myocytes from STZ-induced diabetic rats compared to age-matched healthy controls.

Excitation-Contraction Coupling in Ventricular Myocytes

The arrival of an action potential at a ventricular myocyte causes depolarization of the myocyte plasma membrane and opening of L-type Ca^{2+} channels. A small entry of Ca^{2+} through the Ca^{2+} channels triggers a large release of Ca^{2+} from the SR via the SR Ca^{2+} release channels (Ryanodine receptors). There is a transient rise in intracellular Ca^{2+} concentration, which binds to troponin C and triggers and regulates the process of myocyte contraction. The process of myocyte relaxation takes place when Ca^{2+} is pumped back into the SR via the SERCA pump and extruded from the myocyte, primarily via the Na^{+}/Ca^{2+} exchanger, and also to lesser extents via the plasma membrane Ca^{2+} ATPase [12-14]. Alterations in intracellular $[Ca^{2+}]_i$ and the mechanisms that control intracellular $[Ca^{2+}]_i$ including L-type Ca^{2+} current, SR

Table 7: *In vivo*ventricular function in the streptozotocin-induced diabetic rat.

Parameter	Dose STZ (mg/kg body weight)	Treatment time	Control vs. STZ	Reference
HR	60 ip	10 d	348 vs. 255 bpm	[40]
	65 iv	24, 27 d	412 vs. 376 bpm, 412 vs. 362 bpm	[7]
	40 ip	28 d	388.63 vs. 339.50 bpm NSD	[36]
	60 ip	4, 22 w	347 vs. 268,316 vs. 266 bpm	[3]
	55 ip	7 w	416.5 vs. 304.8 bpm	[5]
	45-50 ip	7-8 w	401.5 vs. 320.8 bpm	[4]
	60 iv	8 w	390 vs. 311 bpm	[30]
	45 iv	8 w	370.2 vs. 283.9 bpm	[6]
	50 ip	8 w	318.24 vs. 243.80 bpm	[32]
	45	8 w	382 vs. 291 bpm	[37]
	65 iv	8 w	357 vs. 283 bpm	[35]
	60 ip	9 w	346 vs. 267 bpm	[38]
	55 iv	12 w	346 vs. 264 bpm	[9]
	60 ip	12 w	420 vs. 388 bpm NSD	[39]
CO	55 ip	7 w	127.0 vs. 94.5 ml/min	[5]
	45-50 ip	7-8 w	128.4 vs. 93.0 ml/min	[4]
	45 iv	8 w	118.7 vs. 82.3 ml/min	[6]
SV	55 ip	7 w	0.31 vs. 0.31 ml NSD	[5]
	45-50 ip	7-8 w	0.32 vs. 0.29 ml	[4]
	45 iv	8 w	0.32 vs. 0.29 ml NSD	[6]
EF	55 ip	7 w	84.1 vs. 76.5%	[5]
	45-50 ip	7-8 w	84.06 vs. 71.8%	[4]
	50 ip	8 w	NSD	[41]
	45 iv	8 w	83.5 vs. 72.5%	[6]
	50 ip	8 w	84.4 vs. 67.8%	[32]
	45	8 w	85 vs. 70%	[37]
	60 ip	9 w	77.33 vs. 64.80%	[38]
	60 ip	12 w	76.1 vs. 67.7%	[39]
FS	55 ip	7 w	61.7 vs. 51.9%	[5]
	45-50 ip	7-8 w	60.6 vs. 52.9%	[4]
	45 iv	8 w	60.9 vs. 49.3%	[6]
	50 ip	8 w	55.7 vs. 39.6%	[32]
	45	8 w	61 vs. 51%	[37]
	60 ip	9 w	41.0 vs. 30.8%	[38]
	60 ip	12 w	45.4 vs. 37.6%	[39]
LVSP	65 iv	21, 24, 27 d	150 vs.136 mmHg 21 d,150 vs. 131 mmHg 24 d,150 vs. 122 mmHg 27 d	[7]
	40 ip	28 d	136.87 vs. 106.32 mmHg	[36]
	55 ip	7 w	Reduced	[5]
	45	8 w	130 vs. 104 mmHg	[37]
	65 iv	8 w	151 vs. 123 mmHg	[35]
LVDP	65 iv	21, 24, 27 d	2.3 vs. 8.6 mmHg 21 d,9.6 mmHg 24 d,9.8 mmHg 27 d	[7]

	65 ip	21 d	Increased	[42]
	40 ip	28 d	2.38 vs. 6.30 mmHg	[36]
	60 ip	8 w	Increased	[33]
	45	8 w	0.6 vs. 4.8 mmHg	[37]
	65 iv	8 w	3 vs. 19 mmHg	[35]
	60 ip	12 w	Increased	[39]
LVPD (+dP/dt)	65 iv	21, 24, 27 d	Reduced	[7]
	40 ip	28 d	5.71 vs. 3.12 mmHg/ms	[36]
	60 ip	8 w	Reduced	[33]
	60 ip	8 w	Reduced	[31]
	5 ip	8 w	Reduced	[5]
	45	8 w	9753 vs. 5176 mmHg/sec	[37]
	65 iv	8 w	6137 vs. 4332 mmHg/sec	[35]
	60 ip	12 w	Reduced	[39]
LVPR (-dP/dt)	65 iv	21, 24, 27 d	Reduced	[7]
	40 ip	28 d	-4.91 vs. -2.66 mmHg/ms	[36]
	55 ip	7 w	Reduced	[5]
	60 ip	8 w	Reduced	[33]
	60 ip	8 w	Reduced	[31]
	45 ip	8 w	9088 vs. 4723 mmHg/sec	[37]
	65 iv	8 w	5415 vs. 3610 mmHg/sec	[35]
	60 ip	12 w	Reduced	[39]
LVRT	60 ip	8 w	Longer	[31]
LVEDD	55 ip	7 w	6.28 vs. 6.91	[5]
	45-50 ip	7-8 w	6.58 vs. 6.70 mm NSD	[4]
	45 iv	8 w	2.6 vs. 3.6 mm	[6]
	60 ip	12 w	11.67 vs. 7.5 mm	[39]
	55 iv	12 w	6.73 vs. 6.86 mm NSD	[9]
LVESD	55 ip	7 w	2.66 vs. 3.35	[5]
	45-50 ip	7-8 w	2.67 vs. 3.234 mm NSD	[4]
	60 ip	12 w	5.84 vs. 4.1 mm	[39]
	55 iv	12 w	2.52 vs. 2.86 mm NSD	[9]
IVRT	50 ip	8 w	Increased	[32]
	55 iv	12 w	Longer	[9]
IVCT	60 ip	8 w	Longer	[31]
BP	55 iv	8 w	110 vs. 105 mmHg NSD	[45]

HR=Heart rate, CO=Cardiac output, SV=Stroke volume, EF=Ejection fraction, FS=Fractional shortening, LVSP=Left ventricular systolic pressure, LVDP=Left ventricular diastolic pressure, LVPR=Left ventricular rate of pressure relaxation, LVRT=Left ventricle relaxation time, LVEDD=Left ventricular end-diastolic dimension, LVESD=Left ventricular end-systolic dimension, IVRT=Isovolumic relaxation time, IVCT=Isovolumic contraction time, BP=Blood pressure.NSD=No significant difference

Ca^{2+} transport and Na^+/Ca^{2+} exchange might partly underlie the disturbances reported in myocyte shortening.

Calcium Transport in Ventricular Myocytes from the Streptozotocin-Induced Diabetic Rat

The effects of STZ-induced diabetes on intracellular Ca^{2+} are shown in Table 9. Resting $[Ca^{2+}]_i$ was generally unaltered [8,9,11,18,28,43,44,47-49,51,53] but sometimes reduced [15,26,44,52,52,54] in ventricular myocytes from diabetic rats compared to controls. A recent study reported unaltered resting Ca^{2+} in EPI and ENDO myocytes in EPI and ENDO left ventricular myocytes from STZ-induced diabetic rats compared to controls [11]. TPK Ca^{2+} transient was either prolonged [9,17,28,49,55,56] or unaltered [10,16,29,38,43,47,48] in myocytes from diabetic rats. THALF decay of the Ca^{2+} transient was generally prolonged [4-6,8-10,16,17,26,28,29,38,48-52,54-57] in myocytes from diabetic rats compared to controls. A recent study reported prolonged TPK Ca^{2+} transient and prolonged THALF decay of the Ca^{2+} transient in ENDO, but not in EPI left ventricular myocytes from STZ-induced diabetic rat [11]. Amplitude of the Ca^{2+} transient was either unaltered [11,16,18,28,29,43,46-49,53,55] or lowered[4-6,9,15,17,26,27,31,32,37,38,54,56,57] in ventricular myocytes from diabetic rats. In addition, the rate of Ca^{2+}transient development and decay were lower in ventricular myocytes from STZ-induced diabetic rats compared to controls [4-6,9,37]. Collectively, these experiments provide evidence of disturbances in the time course of development and decay of the Ca^{2+}transient and the amplitude of the Ca^{2+} transient in

SciMedCentral

Table 8: Contraction in ventricular myocytes from streptozotocin-induced diabetic rat.

Parameter	Dose STZ (mg/kg body weight)	Treatment time	Control vs. STZ	Reference
CV	60 ip	4-10 w	49.4 vs. 25.3%	[16]
	55 iv	6 w	79.4 vs. 70.4%	[44]
	45-50 ip	7-8 w	70 vs. 55%	[4]
	60 ip	8-12 w	49 vs. 25%	[29]
	55 iv	12 w	69 vs. 60 % NSD	[9]
RCL	100 iv	4-6 d	110 vs. 109 µm NSD	[50]
	65 ip	5-7 d	129 vs. 108 µm	[8]
	65 ip	5-7 d	127 vs. 113 µm	[51]
	65 iv	7 d	95 vs. 103 µm	[52]
	65 iv	7 d	128.9 vs. 113.9 µm LV	[27]
	40 iv	3-4 w	126.4 vs. 121.7 µm NSD	[61]
	55 ip	7 w	110.7 vs. 117.8 µm LV NSD	[5]
	45-50 ip	7-8 w	112.30 vs. 112.83 µm NSD	[4]
	60 ip	8 w	NSD	[65]
	60 ip	8 w	NSD	[66]
	55 iv	8 w	111 vs. 110 µm NSD	[50]
	55 iv	8 w	NSD	[45]
	60 ip	8-12 w	NSD	[29]
	60 ip	8-12 w	131.49 vs. 122.48 µm	[47]
	60 ip	8-12 w	117 vs. 113 µm NSD	[46]
	60 ip	8-12 w	131.49 vs. 122.48 µm	[47]
	60 ip	8-12 w	117 vs. 123 µm NSD	[10]
	60 ip	8-12 w	126 vs. 125 µm NSD	[43]
	60 ip	8-12 w	NSD	[28]
	60 ip	12 w	124.5 vs. 124.4 µm EPI NSD, 119.9 vs 121.7 ENDO NSD LV	[11]
	60 ip	13-24 w	138.80 vs. 136.93 µm NSD	[49]
	60 ip	20 w	134.88 vs. 134.94 µm NSD	[48]
TPK Shortening	100 iv	4-6 d	0.1-2.0 Hz NSD	[50]
	65 ip	5-7 days	117 vs. 131 ms	[8]
	65 ip	5-7 days	119 vs. 181 ms	[51]
	65 iv	7 days	103.3 vs. 97.3 ms NSD	[52]
	55 iv	7 w	Prolonged	[26]
	60 ip	8 w	NSD	[66]
	55 iv	8 w	0.1-2.0 Hz Prolonged	[50]
	55 iv	8 w	Prolonged	[45]
	60 ip	8-12 w	305 vs. 360 ms	[10]
	60 ip	8-12 w	105.5 vs. 137.2 ms	[67]
	60 ip	8-12 w	94 vs. 113 ms	[46]
	60 ip	8-12 w	103 vs. 135 ms	[47]
	60 ip	8-12 w	99 vs. 136 ms	[29]
	60 ip	8-12 w	73 vs. 100 ms	[43]
	60 ip	8-12 w	Prolonged	[28]
	55 iv	12 w	Prolonged	[9]
	60 ip	12 w	83 vs. 107 ms EPI, 90 vs. 110 ms ENDO	[11]
	60 ip	13-24 w	97.4 vs. 123.5 ms	[49]
	60 ip	20 w	98.1 vs. 112.1 ms	[48]
THALF relaxation of shortening	100 iv	4-6 d	Prolonged	[50]
	55 ip	7 w	285.9 vs. 445.8 ms NSD	[5]
	45-50 ip	7-8 weeks	382.60 vs. 472.52 ms	[4]
	60 ip	8 w	NSD	[65]
	60 ip	8 w	NSD	[66]
	55 iv	8 w	Prolonged	[50]
	60 ip	8-12 w	NSD	[10]
	60 ip	8-12 w	46.5 vs. 48.6 ms NSD	[67]
	60 ip	8-12 w	NSD	[29]

	60 ip	8-12 w	NSD	[68]
	60 ip	8-12 weeks	41 vs. 51 ms	[46]
	60 ip	8-12 weeks	37 vs. 48 ms	[43]
	60 ip	8-12 w	NSD	[28]
	55 iv	12 w	Prolonged	[9]
	60 ip	12 w	51 vs. 59 ms EPI NSD, 51 vs. 59 ms ENDO	[11]
	60 ip	13-24 w	55.7 vs. 61.1 ms NSD	[49]
	60 ip	20 w	54.7 vs. 53.8 ms NSD	[48]
Time to 90% relaxation of shortening	65 ip	5-7 d	143 vs. 160 ms	[8]
	65 ip	5-7 days	141 vs. 184 ms	[51]
	65 iv	7 days	104.9 vs 138.5 ms	[52]
Tau relaxation	55 iv	7 w	Prolonged	[26]
	55 iv	8 w	Prolonged	[45]
	55 iv	12 w	Prolonged	[9]
Velocity of shortening (+dL/dt)	100 iv	4-6 days	0.5-2.0 Hz Slowed	[50]
	65 iv	7 d	58 vs 58 µm/s NSD	[52]
	55 iv	7 w	Reduced	[26]
	55 ip	7 w	132.2 vs. 75.0 µm/s	[5]
	45-50 ip	7-8 w	159.44 vs. 74.91 µm/s	[4]
	55 iv	8 w	0.1-2.0 Hz Slowed	[50]
	55 iv	8 w	NSD	[45]
	45	8 w	228.6 vs. 89.9 µm/s	[37]
	55 iv	12 w	Lower	[9]
Velocity of relengthening (-dL/dt)	100 iv	4-6 d	0.1-2.0 Hz Slowed	[50]
	65 iv	7 d	-54 vs. -52 µm/s NSD	[52]
	55 iv	7 w	Reduced	[26]
	55 ip	7 w	117.9 vs. 60.9 µm/s	[5]
	45-50 ip	7-8 w	111.56 vs. 65.21 µm/s	[4]
	55 iv	8 w	0.1-2.0 Hz Slowed	[50]
	55 iv	8 w	NSD	[45]
	45	8 w	186.5 vs. 77.1 µm/s	[37]
	55 iv	12 w	Lower	[9]
AMP of shortening	100 iv	4-6 d	0.1 – 2.0 Hz NSD	[50]
	65 ip	5-7 d	7.5 vs. 8.1% NSD	[8]
	65 ip	5-7 d	7.5 vs. 6.7% NSD	[51]
	65 iv	7 d	5.69 vs. 5.51 %	[52]
	65 iv	7 d	9.6 vs. 7.2 (0.5 Hz), 9.7 vs. 8.7 % (2 Hz) NSD	[27]
	55 ip	7 w	11.4 vs. 8.4 µm	[5]
	55 iv	7 w	Reduced	[26]
	60 ip	8 w	NSD	[65]
	60 ip	8 w	NSD	[66]
	45	8 w	14.3 vs. 9.6 %	[37]
	55 iv	8 w	NSD	[45]
	55 iv	8 w	0.1-2.0 Hz Reduced	[50]
	60 ip	8-12 w	NSD	[43]
	60 ip	8-12 w	9.3 vs. 9.6 % NSD	[10]
	60 ip	8-12 w	NSD	[67]
	60 ip	8-12 w	NSD	[29]
	60 ip	8-12 w	NSD	[47]
	60 ip	8-12 w	NSD	[46]
	60 ip	8-12 weeks	9.3 vs. 9.6 % NSD	[10]
	60 ip	8-12 w	NSD	[28]
	55 iv	12 w	Lower	[9]
	60 ip	12 w	6.0 vs. 6.1 % EPI NSD, 6.3 vs. 6.2 % ENDO NSD	[11]
	60 ip	13-24 w	7.29 vs. 7.32 % NSD	[49]
	60 ip	20 w	7.15 vs. 7.41 % NSD	[48]

CV=Cell viability, RCL=Resting cell length, TPK=Time to peak, THALF=Time to half, AMP=Amplitude.NSD=No significant difference ventricular myocytes from STZ-induced diabetic rats compared to controls.

Sarcoplasmic Reticulum Calcium in Ventricular Myocytes from the Streptozotocin-Induced Diabetic Rat

The effects of STZ-induced diabetes on SR Ca^{2+} transport are shown in Table 10. Rapid application of caffeine stimulates release of Ca^{2+} from the SR and provides a measure of releasable SR Ca^{2+} content [58]. Generally, caffeine-evoked Ca^{2+} transients were reduced [4,5,9,15,17,32,41,44,54,57] or sometimes unaltered [11,16,46] in ventricular myocytes from diabetic rats compared to controls. The rate of rise of the caffeine-evoked Ca^{2+} transient was slower [4,5,9] in diabetic rat. TPK caffeine-evoked Ca^{2+} transient was either prolonged [9] or unaltered [16], while the rate of decay of the caffeine-evoked Ca^{2+} transient was generally decreased [5,9,16,44,46] or sometimes unaltered [30] in diabetic rats compared to controls. In contrast, the THALF decay of the caffeine-evoked Ca^{2+} transient was prolonged [4,9,16,29] in ventricular myocytes from diabetic rats compared to controls. The recovery rate of electrically-evoked Ca^{2+} transients following application of caffeine was generally unaltered [11,15,28] or sometimes increased [46]. SR fractional Ca^{2+} release (electrically-evoked as a fraction of caffeine-evoked Ca^{2+} transient) was unaltered [16,28,46,48] in ventricular myocytes from diabetic rats compared to controls. Ca^{2+}-stimulated ATPase activity was generally decreased [26,41], but sometimes unaltered [7], SR Ca^{2+}ATPase mRNA was reduced [33] and SR Ca^{2+} ATPase protein was generally reduced [9,30,32,39,54] or unaltered [5,37] in diabetic rats compared to controls. Ryanodine receptor (RyR) mRNA was unaltered [4]and RyR protein was either reduced [9,17,32,39,54,56] or unaltered [4-6,37] in diabetic rats compared to controls. Moreover, RyR number of functional receptors was decreased [4] RyR activity was decreased [37] and RyR sensitivity to Ca^{2+} was increased [4,5] in diabetic rats compared to controls. In general, the RyR receptors, which conveyed less current, were more responsive to Ca^{2+}, but instead had reduced threshold for Ca^{2+} activation and displayed gain of function [6]. In addition calsequestrin mRNA and calsequestrin total protein content were either reduced [33]or unaltered [9,59] in diabetic rats compared to controls.

Calcium Sparks in Ventricular Myocytes from the Streptozotocin-Induced Diabetic Rat

Calcium sparks represent SR Ca^{2+} release from clusters of ryanodine receptors. The peak amplitude of sparks was either unaltered [17,57], lower [4,5,41] or increased [39] in myocytes from diabetic rat compared to controls. In addition, the spark frequency was either increased [5,6,17,57], reduced [39,41] or unaltered [4], and the duration of sparks was also unaltered [4,5] or reduced [6] in diabetic rats compared to controls. The TPK amplitude of sparks was either prolonged [17,57] or unaltered [39] and the rate of Ca^{2+} rise was either shorter [4-6] or unaltered [41] in myocytes from diabetic hearts compared to controls. There was also evidence that the THALF decay of sparks were either prolonged [5,17,39,57], or unaltered [6] and SR Ca^{2+} load was reduced [39] in ventricular myocytes from diabetic rats compared to controls.

L-type Calcium Current and Sodium/Calcium Exchange Currents in Ventricular myocytes from the Streptozotocin-Induced Diabetic Rat

The effects of STZ-induced diabetes on L-type Ca^{2+} current and Na^{+}/Ca^{2+} exchange are shown in Table 11 and 12. Ventricular myocyte capacitance, which provides a measure of cell size, has been variously reported as either unaltered [17,57,60], increased [18], or decreased [9] in ventricular myocytes from diabetic rats compared to controls. Entry of Ca^{2+} current via the L-type Ca^{2+} channels provides the primary trigger for SR Ca^{2+} release. The density of L-type Ca^{2+} current across a range of test voltages were either unaltered [2,4,11,57,60,61], or reduced [62,63]in myocytes from diabetic hearts compared to controls. Steady-state inactivation [11,60] and recovery from inactivation [11] are unaltered in ventricular myocytes from diabetic rats compared to controls. Some studies have simultaneously measured L-type Ca^{2+} current and either shortening or Ca^{2+} transients. In these studies, L-type Ca^{2+} current and shortening were reduced [16,29], and L-type Ca^{2+} current was unaltered and Ca^{2+} transient was reduced in myocytes from diabetic rats compared to controls[9,41]. Collectively, these experiments provide strong evidence that L-type Ca^{2+} current may be unaltered or reduced and that changes in L-type Ca^{2+} current may or may not be associated with changes in shortening or Ca^{2+} transient in ventricular myocytes from STZ-induced diabetic rat compared to control. Similarly, the Na^{+}/Ca^{2+} exchange current density was reduced [18,41,63], and the current decay was prolonged in myocytes from diabetic rats compared to controls [63]. These alterations in amplitude and kinetics of current were associated with reduced [18] Na^{+}/Ca^{2+}exchange mRNA and generally reducedNa^{+}/Ca^{2+} exchange protein [9,18,39,54] in diabetic rat hearts compared to controls.

Myocardial Fibrosis in Ventricular Myocytes from the Streptozotocin-Induced Diabetic Rat

During development of DC, which is caused by hyperglycemia, and the resulting changes in contraction *in vivo*, the heart responds by producing the transforming growth factor beta 1, which is an initiator and regulator of myocardial fibrosis. Another factor that is also involved in fibrosis is the connective tissue growth factor. Both factors were increased in STZ-induced diabetic hearts compared to controls [36]. Fibrosis was also enhanced [31] with a marked increase in type 1 collagenin diabetic hearts compared to controls [30].

CONCLUSION

Figure 3 summarizes some of the mechanisms of Ca^{2+} transport that are altered in STZ-induced diabetic rat heart. It is well known that STZ (45-65 mg/kg ip or iv), administered to adult rats, damages pancreatic beta cells and reduces the capacity of these cells to release insulin resulting in hyperglycemia and various other characteristics that are observed in DM. *In vivo*, and to a certain extent in the isolated perfused heart, contractile function, in terms of amplitude and kinetics of contraction, are frequently disturbed in the STZ-induced diabetic rat heart. These contractile disturbances are due to many factors including alterations in cellular Ca^{2+} homeostasis, disorganization of the structure

Table 9: Intracellular calcium in ventricular myocytes from streptozotocin-induced diabetic rat.

Parameter	Dose STZ (mg/kg body weight)	Treatment time	Control vs. STZ	Reference
Resting fluorescence ratio or calcium	100 iv	4-6 d	1.72 vs. 1.59 RU NSD	[50]
	65 ip	5-7 d	1.04 vs. 0.98 RU NSD	[51]
	65 ip	5-7 d	1.04 vs. 1.01 RU NSD	[8]
	65 iv	7 d	1.00 vs. 0.90 RU	[52]
	40 iv	3-4 w	Reduced	[15]
	45 iv	4-6 w	0.306 vs. 0.327 RU NSD	[18]
	50 ip	5 w	Increased	[17]
	50 ip	5 w	0.41 vs. 0.49 RU	[57]
	55 iv	6 w	79 vs. 79 nM NSD	[44]
	55 ip	7 w	83.1 vs. 119.1 nM RU LV	[5]
	55 iv	7 w	Reduced	[26]
	60 ip	8 w	NSD	[65]
	60 ip	8 w	NSD	[66]
	60 ip	8-12 w	1.13 vs. 1.08 RU	[47]
	60 ip	8-12 w	2.10 vs. 2.31RU	[10]
	60 ip	8-12 w	2.29 vs. 2.40 RU	[43]
	60 ip	8-12 w	NSD	[28]
	55 iv	12 w	44 vs. 48 nM	[9]
	60 ip	12 w	0.71 vs. 0.69 EPI NSD, 0.73 vs. 0.73 ENDO NSD LV	[11]
	60 ip	13-24 w	1.19 vs. 1.15 RU NSD	[49]
	65 ip	14 w	Reduced	[54]
	60 ip	20 w	1.13 vs. 1.17 RU NSD	[48]
Rate of Ca rise (+dP/dt)	55 ip	7 w	78.8 vs. 12.4 f.u/s LV	[5]
	45-50 ip	7-8 w	39.4 vs. 9.8 f.au/s	[4]
	45 iv	8 w	98.7 vs. 72.2 f.au/s	[6]
	45	8 w	90.7 vs. 70.7 f.au/s	[37]
	55 iv	12 w	Lower	[9]
Rate of Ca decline (-dP/dt)	55 ip	7 w	3.0 vs. 0.6 s^{-1} LV	[5]
	45-50 ip	7-8 w	3.7 vs. 1.2 s^{-1}	[4]
	45	8 w	280.5 vs. 710.0 f.au/ms	[37]
	55 iv	12 w	Lower	[9]
TPK Ca transient	50 ip	4-5 w	Longer	[56]
	60 ip	4-8 w	NSD	[16]
	50 ip	5 w	Prolonged	[17]
	50 ip	5 w	180 vs. 260 ms	[57]
	45-50 ip	7-8 w	65.0 vs. 200.2 ms	[4]
	60 ip	8 w	NSD	[65]
	60 ip	8 w	NSD	[66]
	60 ip	8-12 w	NSD	[43]
	60 ip	8-12 w	NSD	[10]
	60 ip	8-12 w	NSD	[67]
	60 ip	8-12 w	NSD	[29]
	60 ip	8-12 w	64.1 vs. 74.3 ms NSD	[47]
	60 ip	8-12 w	Prolonged	[28]
	60 ip	9 w	NSD	[38]
	55 iv	12 w	Prolonged	[9]
	60 ip	12 w	56.2 vs. 64.2 EPI ms NSD, 60.6 vs. 71.3 ms ENDO LV	[11]
	60 ip	13-24 w	63.5 vs. 76.9 ms	[49]
	60 ip	20 w	65.5 vs. 76.9 ms NSD	[48]
THALF decay Ca transient	65 ip	5-7 days	130 vs. 170 ms	[8]
	40 iv	3-4 w	108 vs. 139 ms	[15]
	50 ip	4-5 w	Longer	[56]
	60 ip	4-8 w	91.8 vs. 166.5 ms	[16]

	50 ip	5 w	Prolonged	[17]
	50 ip	5 w	500 vs. 640 ms LV	[57]
	50 ip	7 w	231.5 vs. 1076.1 ms LV	[5]
	45-50 ip	7-8 w	193.2 vs. 742.6 ms	[4]
	60 ip	8 w	NSD	[65]
	60 ip	8 w	NSD	[66]
	45 iv	8 w	260.5 vs. 699.1 ms	[6]
	60 ip	8-12 w	NSD	[43]
	60 ip	8-12 w	104.8 vs. 148.4 ms	[67]
	60 ip	8-12 w	Prolonged	[29]
	60 ip	8-12 w	NSD	[47]
	60 ip	8-12 w	215 vs. 267 ms	[10]
	60 ip	8-12 w	Prolonged	[28]
	60 ip	9 w	Prolonged	[38]
	55 iv	12 w	Longer	[9]
	60 ip	12 w	189.6 vs. 197.5 ms EPI NSD, 150.3 vs 189.1 ms ENDO LV	[11]
	60 ip	13-24 w	118.4 vs. 160.3 ms	[49]
	60 ip	20 w	115.4 vs. 159.9 ms	[48]
Tau Ca transient	100 iv	4-6 d	0.5 & 1.0 Hz Increased	[50]
	40 iv	3-4 w	89.6 vs. 105.2 ms	[15]
	55 iv	7 w	Elevated	[26]
	50 ip	8 w	Longer	[32]
	55 iv	12 w	Longer	[9]
Fluorescence decay time	65 ip	5-7 d	141 vs. 223 ms	[51]
	65 iv	7 d	248 vs. 320 ms	[52]
	65 ip	14 w	34 vs. 47 ms	[54]
AMP Ca transient	100 iv	4-6 d	2.00 vs. 1.77 RU	[50]
	65 iv	7 d	0.5 Hz 4.78 vs. 4.03 FU 2.0 Hz 3.64 vs. 3.50 FU NSD	[27]
	40 iv	3-4 w	Decreased	[15]
	50 ip	4-5 w	Decreased	[56]
	45 iv	4-6 w	0.377 vs. 0.399 RU NSD	[18]
	60 ip	4-8 w	NSD	[16]
	50 ip	5 w	Reduced	[17]
	50 ip	5 w	0.35 vs. 0.23 AU	[57]
	55 iv	7 w	Reduced	[26]
	55 ip	7 w	3.0 vs. 1.1 f.u LV	[5]
	45-50 ip	7-8 w	2.3 vs. 1.1 f.au	[4]
	60 ip	8 w	NSD	[65]
	60 ip	8 w	NSD	[66]
	50 ip	8 w	Decreased	[32]
	50 ip	8 w	1.82 vs. 1.46 RU	[41]
	45 iv	8 w	4.4 vs. 3.0 fu	[6]
	45	8 w	6.1 vs. 3.8 f.au	[37]
	60 ip	8-12 w	NSD	[43]
	60 ip	8-12 w	NSD	[67]
	60 ip	8-12 w	NSD	[29]
	60 ip	8-12 w	NSD	[47]
	60 ip	8-12 w	NSD	[46]
	60 ip	8-12 w	0.29 vs. 0.39 RU	[10]
	60 ip	8-12 w	NSD	[28]
	60 ip	9 w	Reduced	[38]
	55 iv	12 w	Lower	[9]
	60 ip	12 w	0.17 vs. 0.18 EPI NSD, 0.20 vs. 0.19 RU ENDO NSD LV	[11]
	60 ip	13-24 w	0.42 vs. 0.43 RU NSD	[49]
	65 ip	14 w	0.25 vs. 0.21 RU	[54]
	60 ip	20 w	0.39 vs. 0.47 RU NSD	[48]

RU=Ratio Units, AU=Arbitrary Units, FU=Fluorescence Units, TPK=Time to peak, THALF=Time to half, AMP=Amplitude.NSD=No significant difference

Table 10: Sarcoplasmic reticulum calciumtransport in ventricular myocytes from the streptozotocin-induced diabetic rat.

Parameter	Dose STZ (mg/kg body weight)	Treatment time	Control vs. STZ	Reference
AMP caffeine-evoked Ca transient	40 3-4 w	3-4 w	210.1 vs. 140.8 nM Reduced	[15]
	50ip	5 w	0.42 vs. 0.36 AU	[57]
	50 ip	5 w	Reduced	[17]
	55 6 w	6 w	303 vs. 208 nM. Reduced	[44]
	60 ip	6-8 w	25.7 vs. 25.9 % NSD	[16]
	55 ip	7 w	Reduced LV	[5]
	45-50 ip	7-8 w	0.26 vs. 0.20 RU	[4]
	60 ip	8 w	NSD	[66]
	60 ip	8-12 w	NSD	[46]
	60 ip	8-12 w	NSD	[28]
	60 ip	8 w	NSD	[65]
	50 ip	8 w	Reduced	[32]
	50 ip	8 w	Reduced	[41]
	55 iv	12 w	Reduced	[9]
	60 ip	12 w	EPI ENDO LV NSD	[11]
	65	14 w	0.89 vs. 0.57 RU	[54]
Rate of rise of caffeine-evoked Ca transient	55	7 w	0.014 vs. 0.040 RU/s LV	[5]
	45-50 ip	7-8 w	0.058 vs. 0.048 RU/s	[4]
	55 iv	12 w	Decreased	[9]
TPK caffeine-evoked Ca transient	60 ip	6-8 w	250.3 vs.330.1 ms NSD	[16]
	55 iv	12 w	Prolonged	[9]
Rate of decay of the caffeine-evoked Ca transient	55	6 w	38 vs. 14 nM/sec Decreased	[44]
	60 ip	6-8 w	0.73 vs. 0.56 RU/s	[16]
	60iv	8 w	NSD	[30]
	60 ip	8-12 w	Decreased	[46]
	55 iv	12 w	Decreased	[9]
THALF decline of the caffeine-evoked Ca transient	60	6-8 w	91.8 vs. 156.1 ms	[16]
	55 ip	7 w	17.31 vs. 8.66 s LV	[5]
	45-50 ip	7-8 w	6.70 vs. 11.29 s	[4]
	60 ip	8-12 w	Prolonged	[29]
	55 iv	12 w	0.52 vs. 1.00 s	[9]
Tau rate of decline of the caffeine-evoked Ca transient	45-50 ip	7-8 w	0.116 vs. 0.065 s^{-1}	[4]
	55 iv	12 w	0.54 vs. 1.18 s	[9]
Recovery rate of electrically-evoked Ca transient after caffeine-evoked Ca transient	40 iv	3-4 w	2.26 vs. 3.15 s NSD	[15]
	60 ip	8 w	NSD	[65]
	60 ip	8 w	NSD	[66]
	60 ip	8-12 w	NSD	[28]
	60 ip	8-12 w	Increased	[46]
	60 ip	12 w	ENDO EPI LV NSD	[11]
SR fractional Ca release	60 ip	6-8 w	89.7 vs. 83.5 NSD	[16]
	60 ip	8 w	NSD	[65]
	60 ip	8 w	Increased	[66]
	60 ip	8-12 w	NSD	[28]
	60 ip	8-12 w	NSD	[46]
	60 ip	8-12 w	NSD	[28]
	60 ip	12 w	ENDO NSD EPI Decreased LV	[69]
	60	20 w	NSD	[48]

SR Ca uptake	65 iv	15-27 d	Reduced 21-27 d	[7]
	55 iv	12 w	0.482 vs. 0.149 µM/s	[9]
SR Ca-stimulated ATPase	65 iv	15-27 d	Reduced 21-27 d	[7]
	50 ip	8 w	Decreased	[41]
SR Ca ATPase mRNA	60 ip	8 w	Reduced	[33]
SR Ca ATPase protein (SERCA2)	55 iv	7 w	Reduced	[26]
	55	7 w	LV NSD	[5]
	60 ip	8 w	Reduced	[33]
	50 ip	8 w	Reduced	[41]
	50	8 w	Reduced	[32]
	45	8 w	NSD	[37]
	60 iv	8 w	Reduced	[30]
	60 ip	12 w	Reduced	[39]
	55 iv	12 w	Reduced	[9]
	65 ip	14 w	Reduced	[54]
PLB/PLN protein	55 ip	7 w	NSD LV	[5]
	55 iv	7 w	NSD	[26]
	50 ip	8 w	NSD	[41]
	45	8 w	NSD	[37]
	60 ip	12 w	Increased	[39]
	55 iv	12 w	Increased	[9]
PLB/PLN Ser 16/Thr 17 (Phos)	55 ip	7 w	NSD LV	[5]
	50 ip	8 w	NSD	[41]
	60 ip	12 w	Reduced	[39]
RyR mRNA	45-50 ip	7-8 w	NSD	[4]
RyR protein	50 ip	4-5 w	Reduced	[56]
	50 ip	5 w	Reduced	[17]
	55	7 w	LV NSD	[5]
	45-50 ip	7-8 w	NSD	[4]
	45	8 w	NSD	[6]
	50	8 w	Reduced	[32]
	45	8 w	NSD	[37]
	55 iv	12 w	Reduced	[9]
	65	14 w	Reduced	[54]
RyR2 phosphorylated	50 ip	4-5 w	Increased	[56]
	50 ip	5 w	Reduced	[17]
	55 ip	7 w	Increased LV	[5]
Phos RyR2/RyR2	50 ip	4-5 w	Decreased	[56]
V_{max} Ca uptake into SR	55 iv	12 w	Decreased	[9]
TPK=Time to peak, THALF=Time to half, AMP=Amplitude.NSD=No significant difference				

Table 11: L-type Ca^{2+} current in ventricular myocytes from the streptozotocin-induced diabetic rat.

Parameter	Dose STZ (mg/kg body weight)	Treatment time	Control vs. STZ	Reference
Myocyte capacitance	40 iv	3-4 q	127.4 vs. 127.7 pF NSD	[61]
	40 iv	3-4 w	123 vs. 106 pF NSD	[63]
	45 iv	4-6 w	134.4 vs. 146.8 pF NSD	[18]
	60 iv	4-6 w	196.1 vs. 175.7 pF NSD	[60]
	50 ip	5 w	189.9 vs. 180.6 pF NSD	[57]
	50 ip	5 w	189.9 vs 180.6 pF NSD	[17]
	60 ip	8-12 w	NSD	[29]
	55 iv	12 w	173.82 vs. 112.71 pF	[9]
L-type Ca^{2+} current density	40 iv	3-4 w	Reduced	[63]
	40 iv	3-4 w	NSD	[61]
	60iv	4-6 w	7.5 vs. 8.3 pA/pF NSD	[60]

	60 ip	4-10 w	Reduced	[16]
	50	5 w	NSD	[57]
	45-50	7-8 w	12.0 vs. 11.8 pA/pF NSD	[4]
	60 ip	8 w	11.27 vs. 7.36 pA/pF	[66]
	50 iv	8 w	NSD LV	[2]
	60 ip	8-12 w	Peak current -0.465 vs. –0.304 nA	[67]
	60 ip	12 w	Unaltered EPI ENDO LV	[11]
	65	24-34 w	Reduced	[62]

EPI=Epicardial, ENDO=Endocardial.NSD=No significant difference

Table 12: Sodium/calcium exchange in ventricular myocytes from the streptozotocin-induced diabetic rat.

Parameter	Dose STZ (mg/kg body weight)	Treatment time	Control vs. STZ	Reference
Na^+/Ca^{2+} exchange current density	40 iv	3-4 w	0.49 vs. 0.33 pA/pF	[63]
	45iv	4-6 w	3.50 vs. 1.94 pA/pF	[18]
	50 ip	8 w	Reduced	[41]
Na^+/Ca^{2+} current decay	40 iv	3-4 w	1.59 vs. 3.42 s	[63]
NCX1 protein	45 iv	4-6 w	100 vs. 69 %	[18]
	60 iv	8 w	NSD	[30]
	55 iv	12 w	Reduced	[9]
	65	14 w	Reduced	[54]
	60 ip	12 w	Reduced	[39]
Reversal potential	45 iv	4-6 w	-96 vs. -89 mV	[18]

NSD=No significant difference

of the myocytes, apoptosis, endothelial and mitochondrial dysfunctions, fibrosis and remodeling of the myocardium. In turn, these endogenous processes lead to hemodynamic dysfunction including reduced cardiac output, reduced stroke volume and ejection fraction, reduced percentage of fractional shortening, reduced systolic and increased diastolic pressure, and lower rate of pressure development and decline. In ventricular myocytes, the amplitude of shortening is frequently reduced and the time course of shortening and re-lengthening may be prolonged (delayed contraction) and this can be partly attributed to derangement in cellular Ca^{2+} transport. Alterations in cellular Ca^{2+}transport,including disturbances in L-type Ca^{2+}current(the primary trigger for SR Ca^{2+} release), Na^+/Ca^{2+} exchange current (the major pathway for Ca^{2+} efflux from the cell), SR Ca^{2+} content and SR Ca^{2+} uptake and release mechanism(s) all contribute to contractile dysfunction in the STZ-induced diabetic rat heart.

ACKNOWLEDGMENTS

Grants from the College of Medicine & Health Sciences, United Arab Emirates University, Al Ain; United Arab Emirates University, Al Ain; Sheikh Hamdan Bin Rashid Al Maktoum Award, Dubai; Zayed University, Abu Dhabi.

REFERENCES

1. Lenzen S. The mechanisms of alloxan- and streptozotocin-induced diabetes. Diabetologia. 2008; 51: 216-226.

2. Ding Y, Zou R, Judd RL, Zhong J. Endothelin-1 receptor blockade prevented the electrophysiological dysfunction in cardiac myocytes of streptozotocin-induced diabetic rats. Endocrine. 2006; 30: 121-127.

3. Howarth FC, Jacobson M, Shafiullah M, Adeghate E. Long-term effects of streptozotocin-induced diabetes on the electrocardiogram, physical activity and body temperature in rats. Exp Physiol. 2005; 90: 827-835.

4. Shao CH, Rozanski GJ, Patel KP, Bidasee KR. Dyssynchronous (non-uniform) Ca2+ release in myocytes from streptozotocin-induced diabetic rats. J Mol Cell Cardiol. 2007; 42: 234-246.

5. Shao CH, Wehrens XH, Wyatt TA, Parbhu S, Rozanski GJ, Patel KP, et al. Exercise training during diabetes attenuates cardiac ryanodine receptor dysregulation. J Appl Physiol (1985). 2009; 106:1280-1292.

6. Tian C, Shao CH, Moore CJ, Kutty S, Walseth T, DeSouza C, et al. Gain of function of cardiac ryanodine receptor in a rat model of type 1 diabetes. Cardiovasc Res. 2011; 91: 300-309.

7. Takeda N, Dixon IM, Hata T, Elimban V, Shah KR, Dhalla NS. Sequence of alterations in subcellular organelles during the development of heart dysfunction in diabetes. Diabetes Res and Clin Pract. 1996; 30: 113-122.

8. Ren J, Walsh MF, Hamaty M, Sowers JR, Brown RA. Altered inotropic response to IGF-I in diabetic rat heart: influence of intracellular Ca2+ and NO. Am J Physiol. 1998; 275: H823-H830.

9. Choi KM, Zhong Y, Hoit BD, Grupp IL, Hahn H, Dilly KW, et al. Defective intracellular Ca(2+) signaling contributes to cardiomyopathy in Type 1 diabetic rats. Am J Physiol Heart Circ Physiol. 2002 ;283: H1398-1408.

10. Howarth FC, Adem A, Adeghate EA, Al Ali NA, Al Bastaki AM, Sorour FR, et al. Distribution of atrial natriuretic peptide and its effects on contraction and intracellular calcium in ventricular myocytes from streptozotocin-ind... Peptides. 2005; 26: 691-700.

11. Smail MM, Qureshi MA, Shmygol A, Oz M, Singh J, Sydorenko V, et al. Regional effects of streptozotocin-induced diabetes on shortening and calcium transport in epicardial and endocardial myocytes from rat left ventricle. Physiol Rep. 2016; 4: e13034.

12. Bodi I, Mikala G, Koch SE, Akhter SA, Schwartz A. The L-type calcium

channel in the heart: the beat goes on. J Clin Invest. 2005; 115: 3306-3317.

13. Brette F, Leroy J, Le Guennec JY, Sallé L. Ca2+ currents in cardiac myocytes: Old story, new insights. Prog Biophys Mol Biol. 2006; 91: 1-82.

14. Bers DM1. Cardiac excitation-contraction coupling. Nature. 2002; 415: 198-205.

15. Lagadic-Gossmann D, Buckler KJ, Le Prigent K, Feuvray D. Altered Ca2+ handling in ventricular myocytes isolated from diabetic rats. Am J Physiol. 1996; 270: H1529-537.

16. Bracken N, Howarth FC, Singh J. Effects of streptozotocin-induced diabetes on contraction and calcium transport in rat ventricular cardiomyocytes. Ann N Y Acad Sci. 2006; 1084: 208-222.

17. Yaras N, Bilginoglu A, Vassort G, Turan B. Restoration of diabetes-induced abnormal local Ca2+ release in cardiomyocytes by angiotensin II receptor blockade. Am J Physiol Heart Circ Physiol. 2007; 292: H912-20.

18. Hattori Y, Matsuda N, Kimura J, Ishitani T, Tamada A, Gando S, et al. Diminished function and expression of the cardiac Na+-Ca2+ exchanger in diabetic rats: implication in Ca2+ overload. J Physiol. 2000; 527: 85-94.

19. White FR. Streptozotocin. Cancer Chemother Rep. 1963; 30: 49-53.

20. Schein PS, Cooney DA, Vernon ML. The use of nicotinamide to modify the toxicity of streptozotocin diabetes without loss of antitumor activity. Cancer Res. 1967; 27: 2324-2332.

21. Rerup CC. Drugs producing diabetes through damage of the insulin secreting cells. Pharmacol Rev. 1970; 22: 485-518.

22. Weiss RB. Streptozocin: a review of its pharmacology, efficacy, and toxicity. Cancer Treat Rep. 1982; 66: 427-438.

23. Szkudelski T. The mechanism of alloxan and streptozotocin action in B cells of the rat pancreas. Physiol Res. 2001; 50: 537-546.

24. Belcastro AN, Maybank P, Rossiter M, Secord D. Effect of endurance swimming on rat cardiac myofibrillar ATPase with experimental diabetes. Can J Physiol Pharmacol. 1985; 63: 1202-1205.

25. Howarth FC, Al-Shamsi N, Al-Qaydi M, Al-Mazrouei M, Qureshi A, Chandranath SI, et al. Effects of brain natriuretic peptide on contraction and intracellular Ca2+ in ventricular myocytes from the streptozotocin-induced diabetic rat. Ann N Y Acad Sci. 2006; 1084: 155-165.

26. Norby FL, Wold LE, Duan J, Hintz KK, Ren J. IGF-I attenuates diabetes-induced cardiac contractile dysfunction in ventricular myocytes. Am J Physiol Endocrinol Metab. 2002; 283: E658-E666.

27. Cagalinec M, Waczulíková I, Uličná O, Chorvat D Jr. Morphology and contractility of cardiac myocytes in early stages of streptozotocin-induced diabetes mellitus in rats. Physiol Res. 2013; 62: 489-501.

28. Howarth FC, Qureshi MA, White E. Effects of hyperosmotic shrinking on ventricular myocyte shortening and intracellular Ca(2+) in streptozotocin-induced diabetic rats. Pflugers Arch. 2002; 444: 446-51.

29. Bracken NK, Woodall AJ, Howarth FC, Singh J. Voltage-dependence of contraction in streptozotocin-induced diabetic myocytes. Mol Cell Biochem. 2004; 261: 235-243.

30. Zhang L, Ward ML, Phillips AR, Zhang S, Kennedy J, Barry B, et al. Protection of the heart by treatment with a divalent-copper-selective chelator reveals a novel mechanism underlying cardiomyopathy in diabetic rats. Cardiovasc Diabetol. 2013; 12:123.

31. Delucchi F, Berni R, Frati C, Cavalli S, Graiani G, Sala R, et al. Resveratrol treatment reduces cardiac progenitor cell dysfunction and prevents morpho-functional ventricular remodeling in type-1 diabetic rats. PLoS One. 2012; 7: e39836.

32. Kranstuber AL, Del Rio C, Biesiadecki BJ, Hamlin RL, Ottobre J, Gyorke S, et al. Advanced glycation end product cross-link breaker attenuates diabetes-induced cardiac dysfunction by improving sarcoplasmic reticulum calcium handling. Front Physiol. 2012; 3: 292.

33. Cheng YS, Dai DZ, Dai Y, Zhu DD, Liu BC. Exogenous hydrogen sulphide ameliorates diabetic cardiomyopathy in rats by reversing disordered calcium-handling system in sarcoplasmic reticulum. J Pharm Pharmacol. 2016; 68: 379-388.

34. Galderisi M, Celentano A, Tammaro P, Garofalo M, Mureddu GF, de Divitiis O. Hypertension and arrhythmias: effects of slow-release nicardipine vs chlorthalidone: a double-blind crossover study. Int J Clin Pharmacol Ther Toxicol. 1990; 28: 410-415.

35. Afzal N, Ganguly PK, Dhalla KS, Pierce GN, Singal PK, Dhalla NS. Beneficial effects of verapamil in diabetic cardiomyopathy. Diabetes. 1988; 37: 936-942.

36. Liu Y, Qi H, Wang Y, Wu M, Cao Y, Huang W, et al. Allicin protects against myocardial apoptosis and fibrosis in streptozotocin-induced diabetic rats. Phytomedicine. 2012; 19: 693-698.

37. Moore CJ, Shao CH, Nagai R, Kutty S, Singh J, Bidasee KR. Mol Cell Biochem. 2013; 376:121-1 35.

38. da Silva MF, Natali AJ, da SE, Gomes GJ, Teodoro BG, Cunha DN, et al. Attenuation of Ca2+ homeostasis, oxidative stress, and mitochondrial dysfunctions in diabetic rat heart: insulin therapy or aerobic exercise? J Appl Physiol(1985). 2015; 119: 148-156.

39. Zhao SM, Wang YL, Guo CY, Chen JL, Wu YQ. Progressive decay of Ca2+ homeostasis in the development of diabetic cardiomyopathy. Cardiovasc Diabetol. 2014; 13: 75.

40. Howarth FC, Jacobson M, Naseer O, Adeghate E. Short-term effects of streptozotocin-induced diabetes on the electrocardiogram, physical activity and body temperature in rats. Exp Physiol. 2005; 90: 237-245.

41. Lacombe VA, Viatchenko-Karpinski S, Terentyev D, Sridhar A, Emani S, Bonagura JD, et al. Mechanisms of impaired calcium handling underlying subclinical diastolic dysfunction in diabetes. Am J Physiol Regul Integr Comp Physiol. 2007; 293: R1787-R1797.

42. Liu Z, Cai H, Zhu H, Toque H, Zhao N, Qiu C, et al. Protein kinase RNA-like endoplasmic reticulum kinase (PERK)/calcineurin signaling is a novel pathway regulating intracellular calcium accumulation ... Cell Signal. 2014; 26: 2591-2600.

43. Howarth FC, Qureshi MA. Effects of carbenoxolone on heart rhythm, contractility and intracellular calcium in streptozotocin-induced diabetic rat. Mol Cell Biochem. 2006; 289: 21-29.

44. Yu JZ, Quamme GA, McNeill JH. Altered [Ca2+]i mobilization in diabetic cardiomyocytes: responses to caffeine, KCl, ouabain, and ATP. Diabetes Res Clin Pract. 1995; 30: 9-20.

45. Wold LE, Relling DP, Colligan PB, Scott GI, Hintz KK, Ren BH, et al. Characterization of contractile function in diabetic hypertensive cardiomyopathy in adult rat ventricular myocytes. J Mol Cell Cardiol. 2001; 33: 1719-1726.

46. Rithalia A, Qureshi MA, Howarth FC, Harrison SM. Effects of halothane on contraction and intracellular calcium in ventricular myocytes from streptozotocin-induced diabetic rats. Br J Anaesth. 2004; 92: 246-253.

47. Howarth FC, Qureshi A, Singh J. Effects of acidosis on ventricular myocyte shortening and intracellular Ca2+ in streptozotocin-induced diabetic rats. Mol Cell Biochem. 2004; 261: 227-233.

48. Howarth FC, Almugaddum FA, Qureshi MA, Ljubisavljevic M. Effects of varying intensity exercise on shortening and intracellular calcium in ventricular myocytes from streptozotocin (STZ)-induced diabetic rats. Mol Cell Biochem. 2008; 317: 161-167.

49. Howarth FC, Almugaddum FA, Qureshi MA, Ljubisavljevic M. The effects of heavy long-term exercise on ventricular myocyte shortening and intracellular $Ca2^+$ in streptozotocin-induced diabetic rat. J Diabetes Complications. 2010; 24: 278-285.

50. Ren J, Davidoff AJ. Diabetes rapidly induces contractile dysfunctions in isolated ventricular myocytes. Am J Physiol. 1997; 272: H148-H158.

51. Ren J, Walsh MF, Hamaty M, Sowers JR, Brown RA. Augmentation of the inotropic response to insulin in diabetic rat hearts. Life Sci. 1999; 65: 369-380.

52. Ren J, Wold LE, Epstein PN. Diabetes enhances acetaldehyde-induced depression of cardiac myocyte contraction. Biochem Biophys Res Commun. 2000; 269: 697-703.

53. Ha T, Kotsanas G, Wendt I. Intracellular $Ca2^+$ and adrenergic responsiveness of cardiac myocytes in streptozotocin-induced diabetes. Clin Exp Pharmacol Physiol. 1999; 26: 347-353.

54. Lee TI, Chen YC, Kao YH, Hsiao FC, Lin YK, Chen YJ. Rosiglitazone induces arrhythmogenesis in diabetic hypertensive rats with calcium handling alteration. Int J Cardiol. 2013; 165: 299-307.

55. Ishikawa T, Kajiwara H, Kurihara S. Alterations in contractile properties and $Ca2^+$ handling in streptozotocin-induced diabetic rat myocardium. Am J Physiol. 1999; 277: H2185-2194.

56. Okatan EN, Tuncay E, Turan B. Cardioprotective effect of selenium via modulation of cardiac ryanodine receptor calcium release channels in diabetic rat cardiomyocytes through th... J Nutr Biochem. 2013; 24: 2110-2118.

57. Yaras N, Ugur M, Ozdemir S, Gurdal H, Purali N, Lacampagne A, et al. Effects of diabetes on ryanodine receptor Ca release channel (RyR2) and $Ca2^+$ homeostasis in rat heart. Diabetes. 2005; 54: 3082-3088.

58. Varro A, Negretti N, Hester SB, Eisner DA. An estimate of the calcium content of the sarcoplasmic reticulum in rat ventricular myocytes. Pflugers Arch. 1993; 423: 158-160.

59. Howarth FC, Glover L, Culligan K, Qureshi MA, Ohlendieck K. Calsequestrin expression and calcium binding is increased in streptozotocin-induced diabetic rat skeletal muscle though not in cardiac muscle. Pflugers Arch. 2002; 444: 52-58.

60. Arikawa M, Takahashi N, Kira T, Hara M, Saikawa T, Sakata T. Enhanced inhibition of L-type calcium currents by troglitazone in streptozotocin-induced diabetic rat cardiac ventricular myocytes. Br J Pharmacol. 2002; 136: 803-810.

61. Jourdon P, Feuvray D. Calcium and potassium currents in ventricular myocytes isolated from diabetic rats. J Physiol. 1993; 470: 411-429.

62. Wang DW, Kiyosue T, Shigematsu S, Arita M. Abnormalities of K^+ and $Ca2^+$ currents in ventricular myocytes from rats with chronic diabetes. Am J Physiol. 1995; 269: H1288-1296.

63. Chattou S, Diacono J, Feuvray D. Decrease in sodium-calcium exchange and calcium currents in diabetic rat ventricular myocytes. Acta Physiol Scand. 1999; 166: 137-144.

64. Tappia PS, Maddaford TG, Hurtado C, Dibrov E, Austria JA, Sahi N, et al. Defective phosphatidic acid-phospholipase C signaling in diabetic cardiomyopathy. Biochem Biophys Res Commun. 2004; 316: 280-289.

65. Hamouda NN, Qureshi MA, Alkaabi JM, Oz M, Howarth FC. Reduction in the amplitude of shortening and $Ca(2^+)$ transient by phlorizin and quercetin-3-O-glucoside in ventricular myocytes from streptozotocin-induced diabetic rats. Physiol Res. 2016; 65: 239-250.

66. Hamouda NN, Sydorenko V, Qureshi MA, Alkaabi JM, Oz M, Howarth FC. Dapagliflozin reduces the amplitude of shortening and $Ca(2^+)$ transient in ventricular myocytes from streptozotocin-induced diabetic rats. Mol Cell Biochem. 2015; 400: 57-68.

67. Woodall A, Bracken N, Qureshi A, Howarth FC, Singh J. Halothane alters contractility and $Ca2^+$ transport in ventricular myocytes from streptozotocin-induced diabetic rats. Mol Cell Biochem. 2004; 261: 251-261.

68. Toriyama T, Yokoya M, Nishida Y, Kawajiri K, Takahashi H, Kawahara H. [Increased incidence of coronary artery disease and cardiac death in elderly diabetic nephropathy patients undergoing chronic hemodialysis therapy]. J Cardiol. 2000; 36: 165-171.

69. Campbell SG, Flaim SN, Leem CH, McCulloch AD Mechanisms of transmurally varying myocyte electromechanics in an integrated computational model. Philos Trans A Math Phys Eng Sci. 2008; 366: 3361-3380.

Cite this article

Howarth FC, AlKury L, Smail M, Qureshi MA, Sydorenko V, et al. (2017) Effect of Streptozotocin-Induced Type 1 Diabetes Mellitus on Contraction and Calcium Transport in the Rat Heart. JSM Diabetol Manag 2(1): 1004.